

ANISOTROPIC PERMITTIVITY EXTRACTION FROM PHASE PROPAGATION MEASUREMENTS USING AN ANISOTROPIC FULL-WAVE GREEN'S FUNCTION SOLVER FOR COPLANAR FERROELECTRIC THIN FILM DEVICES

Clifford M. Krowne, Steven W. Kirchoefer, and Jeffrey M. Pond
 Microwave Technology Branch, Electronics Science & Technology Division
 Naval Research Laboratory, Washington, DC 20375-5347

Abstract – Here a full-wave spectral domain integral equation technique is used to study double substrate layer coplanar devices with the ferroelectric thin film adjacent to the conductor guiding interfacial surface. The Green's function is used in the anisotropic situation for anisotropic permittivities. In examining specific laboratory data, going from unbiased static electric field to the biased case, the permittivity tensor is allowed to go from a unity tensor to a uniaxial one.

I. INTRODUCTION

Determination of ferroelectric thin film permittivities has relied upon the measurement of interdigital capacitor values at several hundred MHz to a few GHz [1], [2]. This is a reasonably reliable way to assess the actual permittivity values. However, it would be nice to be able to extract out the permittivity values when the frequency increases significantly, and this appears to be promising for transmission line devices which rely upon wave propagation down a length of uniform transmission line structure [3].

Here we will report on the theoretical procedure to extract out the tensor aspects of the permittivity of the ferroelectric, due to either intrinsic or imposed anisotropy, the simulation technique developed relying upon using a full-wave spectral domain integral equation method using an anisotropic Green's function [4], [5], and preliminary numerical results based upon recent fabricated and measured devices made from $\text{Ba}_x\text{Sr}_{1-x}\text{TiO}_3$ material.

II. FERROELECTRIC PERMITTIVITY TENSOR

In general, assuming the crystalline principal axes of the ferroelectric film are oriented in the coordinate directions, the permittivity tensor $\bar{\bar{\epsilon}}$ looks like

$$\bar{\bar{\epsilon}}(0) = \begin{bmatrix} \epsilon_{xx}(0) & 0 & 0 \\ 0 & \epsilon_{yy}(0) & 0 \\ 0 & 0 & \epsilon_{zz}(0) \end{bmatrix} \quad (1)$$

in the unbiased situation, i.e., $E_{\text{bias}} = 0$. When bias is applied, $\bar{\bar{\epsilon}}$ becomes

$$\bar{\bar{\epsilon}}(E_{\text{bias}}) = \begin{bmatrix} \epsilon_{xx}(E_{\text{bias}}) & 0 & 0 \\ 0 & \epsilon_{yy}(E_{\text{bias}}) & 0 \\ 0 & 0 & \epsilon_{zz}(E_{\text{bias}}) \end{bmatrix} \quad (2)$$

Each tensor $\bar{\bar{\epsilon}}$ element can be a function of each of the three bias field components $E_{i,\text{bias}}$ where $i = x, y, z$. If we assume, for simplicity, diagonal functional projection of the bias field components onto the permittivity tensor $\bar{\bar{\epsilon}}$ elements, then we find

$$\bar{\bar{\epsilon}}(E_{\text{bias}}) = \begin{bmatrix} \epsilon_{xx}(E_{x,\text{bias}}) & 0 & 0 \\ 0 & \epsilon_{yy}(E_{y,\text{bias}}) & 0 \\ 0 & 0 & \epsilon_{zz}(E_{z,\text{bias}}) \end{bmatrix} \quad (3)$$

This is a form simple enough to allow unique determination of the permittivity tensor $\bar{\bar{\epsilon}}$ elements from propagation phase constant β data.

III. COPLANAR PERMITTIVITY TENSOR FORMS

Using the hexagonal perovskite crystalline form for $\text{Ba}_x\text{Sr}_{1-x}\text{TiO}_3$ material, with the c-axis parallel to the y-axis and having different properties than in the a- and b- axes directions parallel to the xz- plane and having the same effects, the tensor $\bar{\bar{\epsilon}}$ looks uniaxial in the unbiased case,

$$\bar{\bar{\epsilon}}(0) = \begin{bmatrix} \epsilon_{xx}(0) & 0 & 0 \\ 0 & \epsilon_{yy}(0) & 0 \\ 0 & 0 & \epsilon_{xx}(0) \end{bmatrix} \quad (4)$$

This $\epsilon_{xx} = \epsilon_{zz}$ equality is broken under bias in the coplanar device, where for the thin films under consideration, $E_{\text{bias}} \approx E_{x,\text{bias}}\hat{x}$ is a reasonable

approximation [6]. Thus the ferroelectric effect makes $\bar{\bar{\epsilon}}$ become

$$\bar{\bar{\epsilon}}(E_{\text{bias}}) = \begin{bmatrix} \epsilon_{xx}(E_{x, \text{bias}}) & 0 & 0 \\ 0 & \epsilon_{yy}(0) & 0 \\ 0 & 0 & \epsilon_{zz}(0) \end{bmatrix} \quad (5)$$

In this form, the permittivity tensor is biaxial.

In order to make the extraction of the tensor element values simple and unique, we impose the condition of isotropy upon the unbiased tensor $\bar{\bar{\epsilon}}$ in (4) to give

$$\bar{\bar{\epsilon}}(0) = \begin{bmatrix} \epsilon(0) & 0 & 0 \\ 0 & \epsilon(0) & 0 \\ 0 & 0 & \epsilon(0) \end{bmatrix} \quad (6)$$

When this done, the value of $\beta_{\text{th}}(0)$ is iterated until the phase propagation constants determined experimentally and numerically agree, that is until $\beta_{\text{th}}[\epsilon(0)] = \beta_{\text{exp}}$. Once this value is on hand, it is assigned to the yy and zz tensor $\bar{\bar{\epsilon}}$ elements in (5) so that $\epsilon_{yy} = \epsilon_{zz} = \epsilon(0)$, converting (5) into

$$\bar{\bar{\epsilon}}(E_{x, \text{bias}}) = \begin{bmatrix} \epsilon_{xx}(E_{x, \text{bias}}) & 0 & 0 \\ 0 & \epsilon(0) & 0 \\ 0 & 0 & \epsilon(0) \end{bmatrix} \quad (7)$$

Once (7) is available, the process of repeated iteration with the unknown to be found, can be started. The iteration process stops when $\beta_{\text{th}}[\epsilon(E_{x, \text{bias}})] = \beta_{\text{exp}}$ has been satisfied.

IV. NUMERICAL EXTRACTION OF TENSOR ELEMENTS

Figures 1 and 2 show the geometry of the thin film structures simulated using the full-wave code. The first structure uses $\text{Ba}_x\text{Sr}_{1-x}\text{TiO}_3$ with a compositional ratio of $x = 0.5$ over a MgO substrate. The second structure has a compositional ratio of $x = 0.6$ over a LaAlO_3 substrate. Both structures have the same size enclosure consisting of perfect electric walls. Box width is $b = 174 \mu\text{m}$, with substrate, ferroelectric film and air region thicknesses being $h_1 = 508 \mu\text{m}$, $h_2 = 0.5 \mu\text{m}$, and $h_3 = 174 \mu\text{m}$. Relative dielectric constants of the substrates are $\epsilon_{\text{sub}} = 9.65$ and $\epsilon_{\text{sub}} = 23.5$ for respectively MgO and a LaAlO_3 . The center strip width $w_s = 6.4 \mu\text{m}$ and slot gap size $w_g = 5.5 \mu\text{m}$ for the film over MgO substrate. These numbers are considerably larger for

the film over LaAlO_3 , being $w_s = 32.76 \mu\text{m}$ and $w_g = 16.4 \mu\text{m}$.

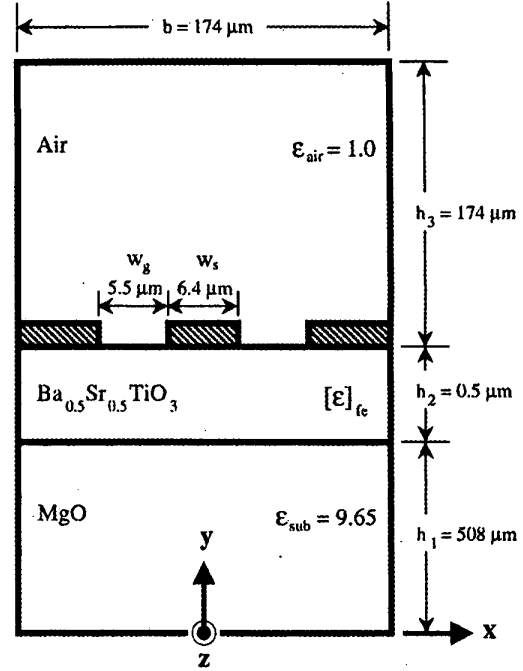


Fig. 1. Computational BST Structure on MgO.

Figure 3 shows a typical phase angle measurement for s_{21} , θ_{21} over the frequency range 0 – 20 GHz, giving the cumulative phase angle seen by the propagating wave traveling through the device made with MgO. The device prepared over MgO had a length of $L = 0.85 \text{ cm}$, whereas the device made with LaAlO_3 had $L = 1.00 \text{ cm}$. Measured θ_{21} on a network analyzer has $-180 \leq \theta_{21} \leq 180$, so the curves in Fig. 3 have been appropriately modified by the formula $\theta_{21, \text{new}} = \theta_{21, \text{old}} \pm \text{mod } 360$. Four bias voltage curves are shown here, $V_{\text{bias}} = 0, 10, 20, 30,$ and 40 V (measurements were also made at the reverse voltages, but they are not provided, nor necessary for the analysis to follow).

To make comparison to the simulation results available from the full-wave code, θ_{21} is converted into a normalized propagation constant. This is done by using the simple formula

$$\bar{\beta} = \theta_{21} / [Lk_0] \quad (8)$$

where $k_0 =$ free space propagation constant.

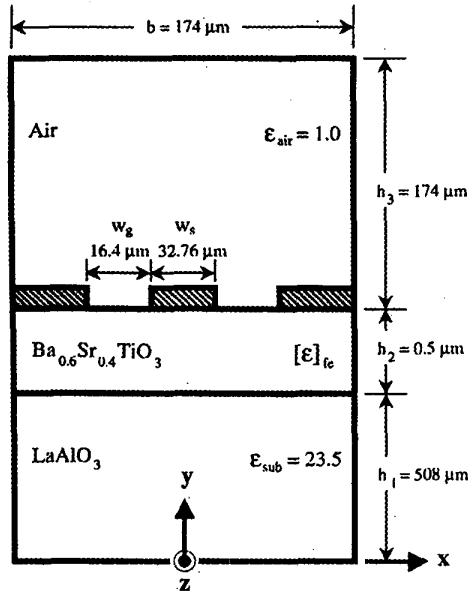


Fig. 2. Computational BST Structure on LAO.

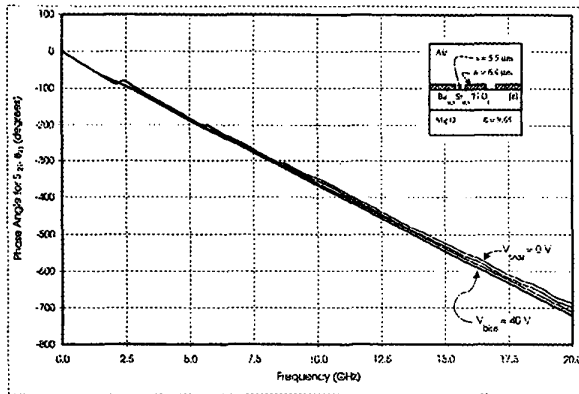


Fig. 3. Phase angle vs frequency for BST thin film MgO device.

These new results are plotted in Figure 4 which shows the two cases $V_{bias} = 0 \text{ V}$ and 40 V . Permittivity extraction method discussed in the last section, based upon (6) and (7), has been applied at 10 GHz on the figure. Top curve for $V_{bias} = 0 \text{ V}$ has a higher slowing $\beta = 3.614$ than the lower curve and we expect its nominal dielectric constant value to be bigger. This is the case as seen from the

determined scalar permittivity value $\epsilon(0) = 123.9$. For the lower curve, $\beta = 3.413$ which yields a permittivity tensor $\bar{\epsilon}$ of

$$\bar{\epsilon}(V_{bias} = 40 \text{ V}) = \begin{bmatrix} 100.2 & 0 & 0 \\ 0 & 123.9 & 0 \\ 0 & 0 & 123.9 \end{bmatrix} \quad (9)$$

Electric field value associated with this tensor solution is found from $E_{x, bias} = V_{bias}/w_g = 47.06 \text{ V/cm}$. It is the electric field value that is the fundamental quantity, not potential difference, since it directly affects the permittivity behavior of the ferroelectric material film.

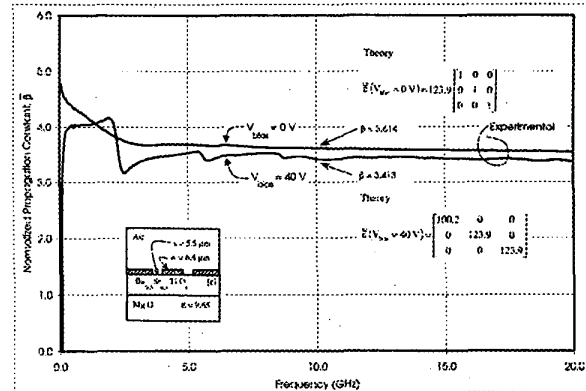


Fig. 4. Dispersion diagram for BST thin film device.

Obviously, it is possible to do the previous calculation at each measured frequency point, allowing a plot of the $\bar{\epsilon}$ tensor elements. Because it is the ϵ_{zz} element that varies, it alone can be plotted versus frequency. Its value will be fairly flat since the curves in Fig. 3 are fairly flat. Variation over f will be due to experimental error, small film material variation over the device surface, and unwanted external and extraneous circuit effects. Because the coplanar device at these dimensions is an extremely low dispersive structure, we do not expect fundamental frequency variation behavior unless the material itself displays such behavior. It is possible to incorporate such material dispersive behavior into the $\bar{\epsilon}$ tensor, although we have not done that in this paper.

Finally, in Figure 5 is shown the results for the device made with a LaAlO_3 substrate. Dielectric constant is much higher for this device with the scalar permittivity $\epsilon(0) = 723.0$ found from

$\bar{\beta}_{th}[\varepsilon(0)] = \bar{\beta}_{exp}$ at $V_{bias} = 0$ V. Solution was obtained as the upper flat line indicated in the Fig. 4, while the experimental curve displays some mild oscillatory character. (Note also that this line is the rms average over the band of the experimental

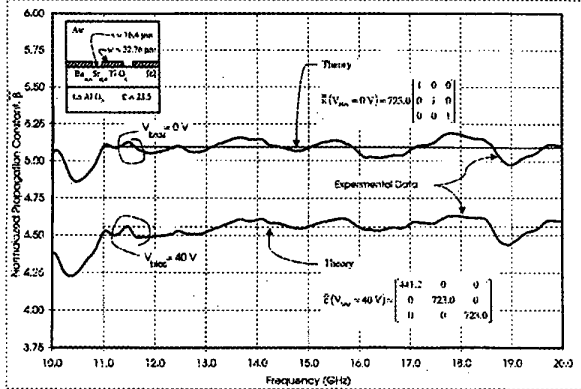


Fig. 5. Dispersion diagram for BST thin film LAO device.

data.) The theoretical $\bar{\beta}_{th}$ goes through the average value of the experimental data $\bar{\beta}_{exp}$ over the frequency range studied. For the lower curve where $V_{bias} = 40$ V ($E_{x, bias} = 40$ V/cm), the permittivity tensor $\bar{\varepsilon}$ is found to be

$$\bar{\varepsilon}(V_{bias} = 40 \text{ V}) = \begin{bmatrix} 441.2 & 0 & 0 \\ 0 & 723.0 & 0 \\ 0 & 0 & 723.0 \end{bmatrix} \quad (10)$$

V. CONCLUSION

A theoretical procedure for determining the permittivity properties of thin film ferroelectric devices has been given. This procedure is to be used in conjunction with a full-wave field solver for extracting out the isotropic and anisotropic behavior of the thin ferroelectric film. A full-wave spectral domain integral equation code with an anisotropic Green's function has been used to find the permittivity values for two ferroelectric thin film devices operated in the microwave frequency regime. Tensor solutions for these devices have been given.

ACKNOWLEDGMENTS

Maurice Daniel of DCS Corporation, Alexandria, VA, contributed to the software work in the code development and to simulation runs. This work has been partially supported by the Office of Naval Research (ONR) and the Defense Advanced Projects Agency (DARPA) in their Frequency Agile Materials for Electronics (FAME) program. Particular thanks goes to Dr. Stuart A. Wolf of DARPA for encouraging this research.

REFERENCES

- [1] S. W. Kirchoefer, J. M. Pond, A. C. Carter, W. Chang, K. K. Agarwal, J. S. Horwitz, and D. B. Chrisey, "Microwave Properties of $Sr_{0.5}Ba_{0.5}TiO_3$ Thin-Film Interdigitated Capacitors," *Microwave & Optical Tech. Letts.*, vol. 18, pp. 168 – 171, June 20, 1998.
- [2] Ferroelectric/Ferrite Tunable Phase Shifters, *Intern. Microwave Th. & Tech. Symp.*, S. W. Kirchoefer, J. M. Pond, H. S. Newman, W.-J. Kim, and J. S. Horwitz, this digest.
- [3] F. W. Van Keuls, C. H. Mueller, F. A. Miranda, and R. R. Romanofsky, C. L. Canedy, S. Aggarwal, T. Venkatesan, R. Ramesh, J. S. Horwitz, W. Chang, and W. J. Kim, "Room Temperature Thin Film $Ba_xSr_{1-x}TiO_3$ Ku-Band Coupled Microstrip Phase Shifters: Effects of Film Thickness, Doping, Annealing and Substrate Choice," *IEEE Microwave Theory Tech. Symp. Dig.*, pp. 737 – 740, June 1999.
- [4] C. M. Krowne, "Fourier Transformed Matrix Method of Finding Propagation Characteristics of Complex Anisotropic Layered Media," *IEEE Trans. Microwave Theory Tech.*, vol. 32, pp. 1617 – 1625, Dec. 1984.
- [5] A. A. Mostafa, C. M. Krowne, K. A. Zaki, "Numerical Spectral Matrix Method for Propagation in General Layered Media: Application to Isotropic and Anisotropic Substrates," *IEEE Trans. Microwave Theory Tech.*, vol. MTT-35, pp. 1399-1407, Dec. 1987.
- [6] C. M. Krowne, "Nonlinear Electromagnetic Wave Propagation in Ferroelectric Integrated Structures," *Microwave Optical Techn. Letts.*, vol. 17, pp. 213 - 225, Feb. 20 1998.